Adel Saki | Mohssen Moazzen | Roland Oberhänsli

Mineral chemistry and thermobarometry of the staurolite-chloritoid schists from Poshtuk, NW Iran

Suggested citation referring to the original publication:
Geological Magazine 149 (2012) 6, pp. 1077–1088
DOI https://doi.org/10.1017/S0016756812000209
ISSN (print) 0016-7568
ISSN (online) 1469-5081

Geol. Mag. **149** (*6*), *2012, pp. 1077–1088. © Cambridge University Press 2012*
doi:10.1017/S0016756812000209

Mineral chemistry and thermobarometry of the staurolite-chloritoid schists from Poshtuk, NW Iran

ADEL SAKI*†, MOHSSEN MOAZZEN‡ & ROLAND OBERHÄNSLI§

*Department of Geology, Shahid Chamran University of Ahvaz, Iran
‡Department of Geology, University of Tabriz, 51664, Tabriz, Iran
§Institute of Earth & Environmental Sciences, Potsdam University, Karl-Liebknecht-Strasse 24, 14476 Potsdam, Germany

(*Received* 13 June 2011; *accepted* 23 February 2012; *first published online* 17 May 2012)

Abstract – The Poshtuk metapelitic rocks in northwestern Iran underwent two main phases of regional and contact metamorphism. Microstructures, textural features and field relations indicate that these rocks underwent a polymetamorphic history. The dominant metamorphic assemblage of the metapelites is garnet, staurolite, chloritoid, chlorite, muscovite and quartz, which grew mainly syntectonically during the later contact metamorphic event. Peak metamorphic conditions of this event took place at 580 °C and ~ 3–4 kbar, indicating that this event occurred under high-temperature and low-pressure conditions (HT/LP metamorphism), which reflects the high heat flow in this part of the crust. This event is mainly controlled by advective heat input through magmatic intrusions into all levels of the crust. These extensive Eocene metamorphic and magmatic activities can be associated with the early Alpine Orogeny, which resulted in this area from the convergence between the Arabian and Eurasian plates, and the Cenozoic closure of the Tethys oceanic tract(s).

Keywords: thermobarometry, HT/LP metamorphism, Poshtuk metapelites, northwestern Iran.

1. Introduction

Low-pressure, high-temperature (LP/HT) metamorphic belts reflect some of the highest thermal perturbations of the upper crust, with average gradients generally between 35 °C and 75 °C km^{-1} at $P < 5$ kbar (Treloar & O'Brien, 1998). Such belts are generally interpreted to result from a transient, enhanced crustal heat flux, possibly derived from advection of heat associated with magma emplacement (e.g. Treloar & O'Brien, 1998). For the average gradients listed above, an assumed Moho temperature of 650 °C requires that crustal thickness should be only 10–20 km during LP/HT metamorphism, which implies crustal thinning.

One of the aims of metamorphic petrology is to gain information about the pressure and temperature histories of metamorphic areas through the use of mineral equilibrium. Chemical analyses of minerals assumed to be in equilibrium have been used in conjunction with geobarometers and geothermometers to estimate the pressure (P) and temperature (T) conditions attained at or near the peak of metamorphism (e.g. Richards & Collins, 2002; Ricardo & Martínez Catalán, 2003). Recognition and characterization of superimposed metamorphic episodes, either during a continuous polyphase metamorphic P–T path (e.g. subduction–collision–exhumation; e.g. Otaa, Terabayashi & Katayama, 2004) or during repeated cycles of polymetamorphism (e.g. 'Caledonian'–Hercynian/Variscan–Alpine evolution of the Eastern Alps) is critical for the understanding of the tectonic evolution of a metamorphic basement.

The Poshtuk area in the northwest of Iran (Fig. 1a) experienced polyphase metamorphism and magmatism from Palaeoproterozoic to Tertiary times. Tertiary metamorphism and magmatism occurred during the subduction of the Neo-Tethys (Mohajjel, Fergusson & Sahandi, 2003).

The timing of the closure of the Neo-Tethys and the collision between the Arabian plate and the Iranian microcontinent is debated. Berberian & King (1981) and Alavi (1994) favour a Late Cretaceous age for the collision along the Zagros suture. Others envision a Cenozoic age for the continental collision (e.g. Agard *et al*. 2005). Based on palinspastic and plate tectonic reconstructions, McQuarrie *et al*. (2003) suggested that the collision between the Arabian plate and the Iranian microcontinent occurred before 20 Ma at most, in relation to the subduction of the Neo-Tethys. Recent studies by Verdel *et al*. (2007) support the Neogene collision between the Arabian plate and the Iranian microcontinent. Allen & Armstrong (2008) showed that the Arabia–Eurasia collision and the closure of the Tethys oceanic gateway began in the Late Eocene at ~35 Ma, up to 25 million years earlier than in many reconstructions.

There is no published study on the nature of the metamorphism of the pelitic rocks and their deformation in the Poshtuk area so far. This investigation aims to study the type of metamorphism and the deformational phases as well as the relations between these two using the textural relations and mineral chemistry of the metapelitic rocks of the area. This will provide a basis

† Author for correspondence: adel_saki@scu.ac.ir

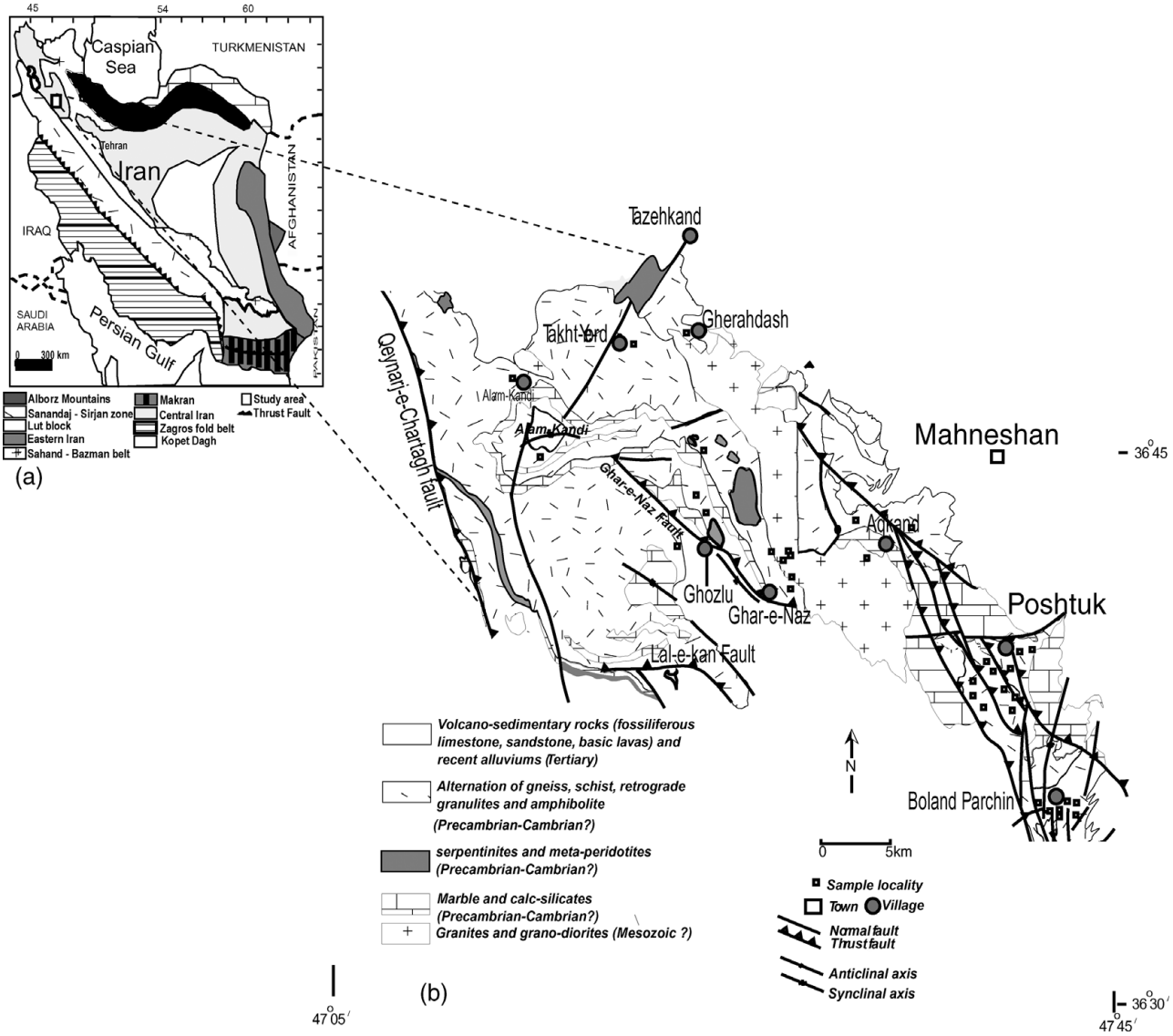

Figure 1. (a) Simplified structural subdivision map of Iran and the locality of the study area (modified from Stocklin & Setudenia, 1972). (b) Geological map of the Mahneshan Complex and Poshtuk sub-area and sample locations.

for further studies on the metamorphic and geodynamic evolution of this part of the Iranian crust.

2. Regional geological setting

The Iranian plateau consists of several continental fragments welded together along the palaeo-oceanic suture zones (Neoproterozoic). These fragments are bordered by major faults. Each fragment shows different sedimentary, stratigraphic, magmatic and metamorphic features. One of these fragments is the continental crust of the Central Iran Zone, which was metamorphosed and intruded by granites and faulted during the Late Precambrian Pan-African Orogeny (Ramezani & Tucker, 2003; Saki, 2010). The Sanandaj–Sirjan zone is a metamorphic belt associated with the Central Iran Zone. This belt extends across Iran in a NW–SE direction (Fig. 1a). Subduction of the Neo-Tethys between the Afro-Arabian plate and the Iranian microplate and subsequent continental collision (during Cretaceous to Early Tertiary times) caused metamorphism and associated magmatism in the Sanandaj–Sirjan Zone (Mohajjel, Fergusson & Sahandi, 2003; Moazzen *et al*. 2004).

The study area is located in the south of the town of Mahneshan, western Zanjan (Fig. 1b). The area is limited to geographical latitude 47° 07′ to 47° 45′ E and longitude 36° 30′ to 37° 00′ N (Fig. 1b).

In the context of the structural subdivisions of Iran, the Poshtuk area has been assigned to various tectonic zones by different workers. It is included in the Central Iran Zone by Nabavi (1976), the Soltanieye–Misho Zone by Eftekhar Nejad (1980) and at the junction of the Central Iran, Alborz–Azerbaijan and Sanandaj–Sirjan zones by Babakhani & Ghalamghash (1990). Recently Alavi (2004) and Gilg *et al*. (2006) have included the study area in the Sanandaj–Sirjan Zone. In the geological map of the area, issued by the Geological Survey of Iran (Babakhani & Ghalamghash, 1990), it is included between the Alborz–Azerbaijan, Central Iran and Sanandaj–Sirjan zones. Similarities in stratigraphy, lithology and age data (relative and isotopic ages) of the

https://doi.org/10.1017/S0016756812000209

Table 1. Representative major (wt %) compositions of metapelitic rocks from the Poshtuk area (bulk rock analyses)

Sample	SiO_2	TiO_2	Al_2O_3	Fe_2O_3	MnO	MgO	CaO	Na_2O	K_2O	P_2O_5	H_2O	CO_2	Sum
1	64.00	1.450	17.50	11.90	0.154	0.60	0.50	0.40	0.80	0.065	2.48	0.10	99.8
2	56.60	1.180	23.00	8.78	0.045	1.08	1.04	0.58	3.86	0.121	0.19	3.23	99.6
3	54.60	1.570	20.50	10.65	0.109	1.90	1.92	1.09	3.02	0.139	3.90	0.26	99.7
4	58.20	0.990	18.95	7.45	0.072	2.83	0.47	1.19	5.99	0.145	2.85	0.56	99.5
5	63.50	0.860	17.45	5.74	0.117	1.63	0.86	1.59	3.32	0.134	3.17	2.05	99.6
6	40.50	1.665	24.93	14.93	0.407	3.92	7.87	1.57	1.33	0.065	1.87	0.13	99.2
7	61.20	0.770	16.55	6.35	0.08	2.35	0.65	1.54	5.05	0.120	0.60	0.20	98.1
8	62.00	0.775	16.60	6.82	0.077	2.15	3.75	3.98	2.06	0.256	0.95	0.14	99.7
9	63.70	0.706	15.82	6.09	0.108	2.06	3.80	3.85	2.15	0.218	1.10	0.17	99.7
10	65.90	0.810	16.90	6.40	0.15	1.85	0.65	1.55	2.47	0.130	0.19	0.15	99.8

protoliths of the Mahneshan and Poshtuk complex and equivalent units from the Central Iran Zone suggest that the Mahneshan Complex has a Neoproterozoic–Early Cambrian age and has experienced the Pan-African Orogeny (e.g. Hajialioghli *et al*. 2007; Moazzen *et al*. 2009). The strips of ultramafic rocks in the Takab Complex can be interpreted as lithospheric remnants of the Proto-Tethyan, which closed during the Pan-African Orogeny (Hajialioghli *et al*. 2007; Saki, 2011). Therefore, it is included in the Central Iran Zone. K–Ar dating of carbonaceous schists in the Zarshuran area (Mehrabi, Yardley & Cann, 1999), apatite U–Th/He data from the Mahneshan area (Stockli *et al*. 2004) and ^{40}Ar–^{39}Ar dating of muscovite schists (Gilg *et al*. 2006), constrain the timing of rapid exhumation of the basement rocks to Early Miocene time (20 Ma). On the geological map of the Mahneshan area, the age of I-type granitoids is attributed to Mesozoic time (late Cimmerian orogenic phase). Recently, Jamshidibadr *et al*. (2011) found two distinct types of granitoids in the Soursat area, to the south of Poshtuk: a type I granitoid, $\sim$ 540 Ma and a type II granitoid, 59.0 $\pm$ 2.7 Ma.

The main regional trend of the rocks is NW–SE, and these rocks were exposed by a young reverse fault (Chartagh Fault). The fault has placed the metamorphic rocks adjacent to the Miocene sediments. The plutonic rocks are intruded into the regional metamorphic rocks.

The Poshtuk metamorphic rocks in northwestern Iran were affected by regional and contact metamorphism. A variety of igneous and metamorphic rocks can be seen in the studied area (Fig. 1b). The metamorphic rocks in the Poshtuk area include garnet-staurolite micaschists, chloritoid-staurolite micaschists, metalimestone, augen-gneisses and amphibolites. The igneous rocks of the area are composed of two types (Saki, 2011): (1) S-type granitoids (anatectic alkali granite) and (2) white to light grey I-type igneous rocks. Samples for this study were collected from the mountains northwest of Poshtuk village. Figure 1b illustrates the sample localities and rock types.

3. Petrography

Petrographic features and mineral assemblages of the metapelitic rocks are described in the following sections. Detailed petrographic studies of thin-sections were carried out on all specimens (40). Table 1 shows mineral assemblages of the Poshtuk metapelitic rocks. Mineral abbreviations are after Kretz (1983). Sample locations are shown in Figure 1b.

The representative mineral assemblages in the studied metapelites of Poshtuk are:

Grt + Ms + Chl + Qtz
Grt + Ms + Ctd + Chl + Qtz
Grt + St + Ms + Ctd + Chl + Qtz
Grt + St + Ms + Chl + Qtz

A polyphase deformation can be considered based on two foliations, S_1 and S_2, and inclusions in the porphyroblasts. Fabrics of D_1 (the first deformational phase) are clearly deformed by D_2 (second and the main deformational phase). D_2 is the most obvious and pervasive deformation in the area. The mylonitic foliation enveloping garnet porphyroblasts, S_2, (formed during the deformation phase D_2) is best seen in samples from the Poshtuk schist (Fig. 2a, b) where it is defined by the parallel alignment of biotite and muscovite (Fig. 2b). S_1 foliation can be seen in crenulation cleavage (Fig. 2c). S_2 is parallel to the axial planes of the micro-folds of intercalated quartz-feldspar-rich and phyllosilicate-rich layers. This foliation represents the main regional foliation and can be recognized throughout all metamorphic zones.

Porphyroblasts that formed during the regional metamorphic phase are usually overprinted (superimposed) by mineral growth associated with contact metamorphism.

4. Regional and contact metamorphism

The mineral assemblage of regional metamorphism, garnet–chlorite (in addition to plagioclase, muscovite, quartz and ilmenite), is inferred from mineral inclusions. Subsequently, the prograde metamorphic phase (contact metamorphism) is characterized by development of new porphyroblasts, including garnet (Grt_1; Fig. 2b), staurolite, chloritoid and chlorite (in addition to plagioclase, muscovite, quartz and ilmenite). This phase is the major contact metamorphic phase in the studied area. This metamorphism overprinted the regional metamorphic assemblages.

https://doi.org/10.1017/S0016756812000209

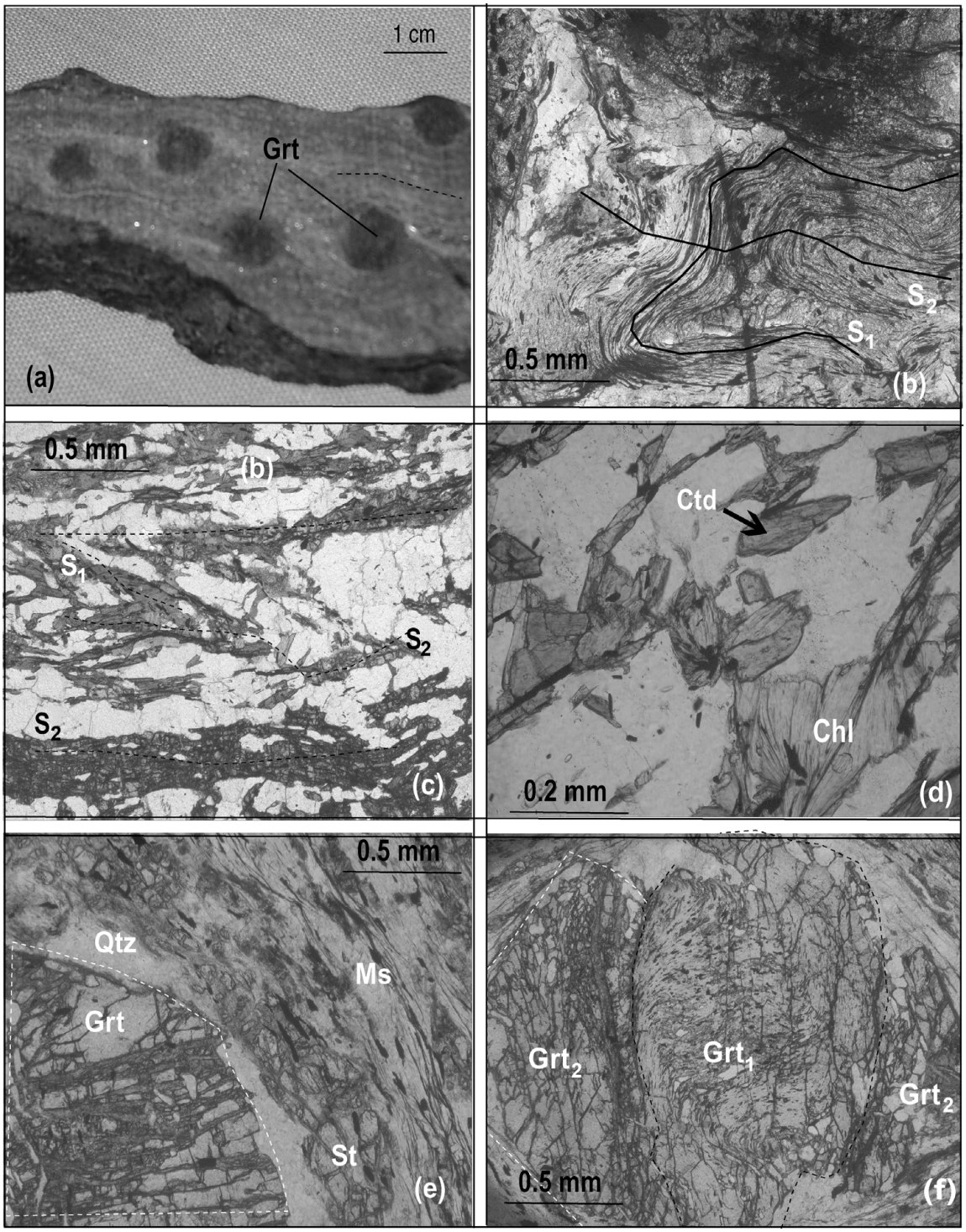

Figure 2. (a) Garnet porphyroblasts (Grt) with 5 to 15 mm diameter are formed in chloritoid schists; hand specimen. (b) D_1 and D_2 deformational phases picked up by S_1 and S_2 schistosities. (c) A schistosity (S_1) is defined by a preferred orientation of muscovite; chloritoid and chlorite is affected by a crenulation schistosity. (d) Chlorite and chloritoid are formed in equilibrium. (e) Staurolite and muscovite nucleated at the margin of garnet. (f) Syntectonic helcitic garnet porphyroblasts (Grt_1) formed during M_2 metamorphism; garnet (Grt_2) is formed during contact metamorphic phase.

4.a. Chlorite and muscovite

Regionally, metamorphic chlorite and muscovite are crystallized in the Poshtuk metapelitic rocks (Fig. 2d). The rock is composed of fine-grained muscovite, chlorite, quartz and porphyroblasts of helicitic garnet and staurolite. A second generation of chlorite and muscovite up to 0.3 mm in size also formed parallel to the S_2 foliation.

4.b. Garnet

The garnet zone consists of medium- and coarse-grained schists (Fig. 2a). Garnet forms euhedral to

https://doi.org/10.1017/S0016756812000209

Table 2. Representative trace (ppm) element compositions of metapelitic rocks from the Poshtuk area (bulk rock analyses)

Sample	Ba	Cr	Ga	Nb	Ni	Rb	Sr	V	Y	Zn	Zr
1	950	120	25	35	36	46	520	203	400	125	370
2	780	121	27	27	39	162	190	154	46	107	215
3	389	133	24	27	50	105	166	198	26	123	231
4	945	123	29	14	55	179	59	155	32	98	204
5	425	99	20	17	45	105	113	128	25	190	225
6	295	248	17	13	139	37	502	320	90	97	537
7	690	260	24.2	14.4	39	182.5	70.7	129	29.9	281	185
8	440	17	19	20	10	41	217	70	34	21	223
9	443	18	16	11	10	35	220	68	28	35	210
10	326	300	21.3	17.3	46	117	108.5	124	26.8	91	232

subhedral, sometimes quartz inclusion-rich porphyroblasts and shows textural zoning (Fig. 2f). Most garnets show two stages of growth: first, garnet with spiral-shaped inclusion fabrics, which developed during syntectonic (S_2) growth (Grt_1 or regional metamorphic garnet); and second, garnet, free of inclusions, which developed during contact metamorphism (Grt_2) (Fig. 2f). Rotated garnet porphyroblasts up to 13 mm in diameter are developed in the Poshtuk schists.

4.c. Staurolite

Staurolite forms porphyroblasts with sizes up to several millimetres in the chloritoid schists. Staurolite commonly nucleated at the margin of garnet or in phyllosilicate-rich layers (Fig. 2e). In Figure 2e, garnet is replaced by staurolite, which in turn is pseudomorphed by muscovite.

4.d. Chloritoid

Chloritoid occurs in the fine-grained rock matrix as lath-shaped crystals, and under the microscope (plain-polarized light) has a blue colour (Fig. 2d). The sample consists of garnet, chloritoid, staurolite (up to 0.5 mm), chlorite and muscovite. Therefore, the main paragenesis in these rocks is: Ctd + Grt + St + Ms + Chl + Qtz.

5. Bulk rock chemistry

Major and trace elements of ten metapelitic rocks of the Poshtuk area were analysed by standard X-ray fluorescence (XRF) methodology using a Philips PW 1480 XRF spectrometer. The analyses are listed in Tables 1 and 2. In the discrimination diagram $\log(Fe_2O_3{}^t/K_2O)$ v. $\log(SiO_2/Al_2O_3)$ after Herron (1988) most of the Mahneshan metapelites plot in the shale field; only two samples plot in the fields of Fe-shale (Fig. 3). Similar results were obtained by using the empirical discrimination ratio $100TiO_2/Zr$ (wt %/ppm) to distinguish between psammitic and pelitic sediments (Garcia, Coelho & Perrin, 1991; Häussinger, Okrusch & Scheepers, 1993). Almost all samples have values above 0.4 and, accordingly, were derived from pelitic sediments, whereas, the remaining samples have a psammitic precursor.

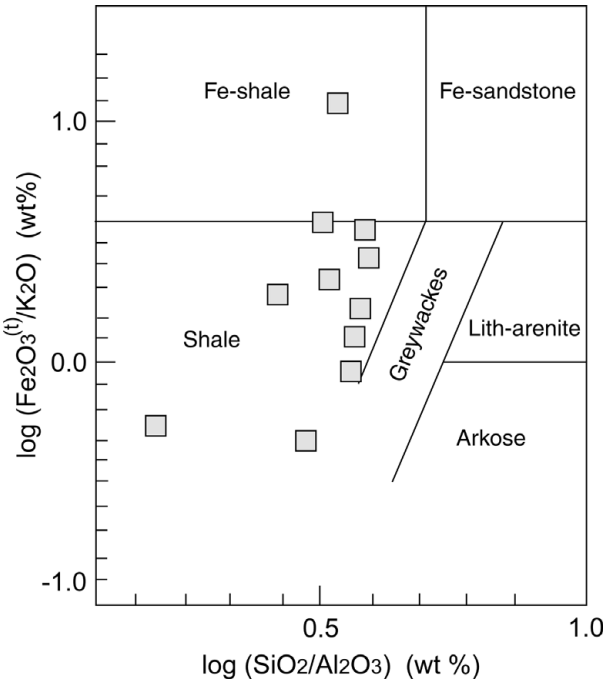

Figure 3. Discrimination diagram log ($Fe_2O_3{}^t/K_2O$) v. log (SiO_2/Al_2O_3) from Herron (1988), showing a predominant shale composition for the Poshtuk metapelites.

6. Mineral chemistry

Major element compositions of chloritoid, muscovite, biotite, garnet, staurolite and plagioclase in selected metapelites were determined by wavelength-dispersive spectrometry using a Cameca SX100 microprobe at the GeoForschungsZentrum (GFZ), Potsdam, Germany. The operational conditions were 15 kV, 10–20 nA specimen current. The analytical spot diameter was set between 3 and 5 μm, keeping the same current conditions. Natural and synthetic standards were used for calibration (Tables 3 and 4). Ferric iron contents in ferromagnesian minerals were calculated using stoichiometric criteria (Droop, 1987).

6.a. Chlorite

Representative analyses of chlorite are shown in Table 3. The oxide totals are between 91.00 and 91.52. The amount of Ti is between 0.01 and 0.04 atoms

https://doi.org/10.1017/S0016756812000209

Table 3. Representative chloritoid, muscovite and chlorite analyses and structural formulae

Mineral	Ctd	Ctd	Ctd	Ms	Ms	Ms	Chl	Chl	Chl	Chl	Chl
	Core										
SiO_2	23.60	23.44	23.45	46.25	46.45	46.70	23.00	23.15	22.98	22.75	23.30
TiO_2	0.00	0.02	0.01	0.18	0.20	0.18	0.08	0.22	0.11	0.14	0.12
Al_2O_3	41.35	41.26	41.10	37.86	37.58	37.52	23.00	23.32	23.32	23.09	23.25
Cr_2O_3	0.07	0.06	0.04	0.03	0.00	0.05	0.06	0.07	0.08	0.09	0.11
Fe_2O_3	1.31	2.10	1.30	1.28	1.24	1.25	1.31	0.81	0.51	0.57	1.11
FeO	26.37	26.16	26.41	0.29	0.28	0.28	36.72	35.45	37.85	39.17	34.96
MnO	0.03	0.00	1.01	0.00	0.01	0.00	0.09	0.07	0.07	0.12	0.02
MgO	1.65	1.70	1.65	0.18	0.27	0.28	7.13	8.19	6.57	5.55	8.58
CaO	0.01	0.02	0.00	0.01	0.00	0.00	0.00	0.00	0.00	0.01	0.00
Na_2O	0.00	0.01	0.00	1.85	1.82	1.65	0.04	0.01	0.01	0.02	0.00
K_2O	0.02	0.00	0.01	8.93	8.92	8.52	0.01	0.01	0.00	0.00	0.00
Totals	94.41	94.76	94.10	97.80	95.75	96.10	91.45	91.30	91.50	91.52	91.00
Structural formulae on a basis of	*12 oxygen atoms*			*11 oxygen atoms*			*28 oxygen atoms*				
Si	0.994	0.986	0.997	2.97	2.98	2.98	2.48	2.47	2.48	2.48	2.48
Ti	0.00	0.00	0.00	0.01	0.01	0.02	0.00	0.02	0.00	0.01	0.01
Al	1.97	1.96	1.96	2.95	2.93	2.94	2.92	2.94	2.97	2.96	2.92
Cr	0.00	0.00	0.00	0.00	0.00	0.00	0.00	0.00	0.00	0.00	0.00
Fe(3+)	0.04	0.06	0.04	0.06	0.06	0.01	0.10	0.06	0.04	0.05	0.09
Fe(2+)	0.89	0.88	0.90	0.01	0.015	0.02	3.31	3.174	3.42	3.57	3.12
Mn	0.00	0.00	0.00	0.00	0.00	0.00	0.00	0.00	0.00	0.01	0.00
Mg	0.10	0.10	0.10	0.01	0.03	0.03	1.14	1.30	1.0.6	0.90	1.36
Ca	0.00	0.00	0.00	0.00	0.00	0.00	0.00	0.00	0.00	0.00	0.00
Na	0.00	0.00	0.00	0.23	0.22	0.20	0.00	0.00	0.00	0.00	0.00
K	0.001	0.00	0.00	0.73	0.73	0.76	0.00	0.00	0.00	0.00	0.00
Totals	4.00	4.00	4.00	6.99	6.98	6.90	10.00	10.00	10.00	10.00	10.00

per formula unit (apfu). The chlorites are Mn-free. Na varies from 0.00 to 0.02 apfu, and K from 0.00 to 0.03 apfu. Substitution of Al^{3+} for Si^{4+} is calculated using the stoichiometric approach after Saad, Bouseil & Kalil (1996). Chlorites are of daphnite type and Fe-rich nature. According to Laird (1988) (Fig. 4a), prograde chlorite compositions plot close to the medium-/low-*P* field.

6.b. Muscovite

Muscovite analyses are listed in Table 3. According to Figure 4b after Lambert (1959), muscovites are rich in the muscovite end-member, and paragonite is the second most important component. The mole fractions of other components are negligible. Reduction in the phengite component of muscovite with metamorphic grade has been described by several authors (e.g. Mather, 1970; Wang, Banno & Takeuchi, 1986; Dempster & Tanner, 1997) in different low-to-medium pressure metamorphic terranes.

6.c. Garnet

Garnet compositions are listed in Table 4. Garnets are Fe-rich with almandine contents varying between 80 and 90 %. Ti is not present or occurs in very low amounts. Figure 4c shows the chemical composition of the analysed garnets in the almandine (Alm), pyrope (Pyp) and grossular+spessartine (Grs+Sps) triangular diagram. Stoichiometry and the Fe^{3+} content of garnet were calculated based on 8 cations and 12 oxygen atoms. The zoning profile shown in Figure 4d is from rim to rim and cuts through the core of the garnet. There is no significant zoning in the garnet.

6.d. Staurolite

Staurolite analyses are listed in Table 4. The number of cations is calculated based on 28 oxygen atoms. Staurolite in some samples has distinctly less MgO ($\approx$ 0.35 %) and ZnO ($\approx$ 0.30 %). The staurolite does not show any significant zoning. Compositional ranges of staurolite in the Fe, Mg and (Mn+Zn) triangular diagrams indicate Fe-staurolite compositions. MnO and ZnO contents are very low. Staurolite shows lower X_{Fe}-values than coexisting garnet.

6.e. Chloritoid

Representative mineral compositions of chloritoids in the studied samples are given in Table 3. The chloritoid formula $(Fe,Mn,Mg)_2Al_4Si_2O_{10}(OH)_4$ was calculated on the basis of 12 oxygen atoms. It is Fe-rich, and the Fe/Mg ratio is much higher than in the coexisting chlorite. Figure 4e illustrates the composition of chloritoids in Al+Fe^{3+}, Fe^{2+}+Mn and Mg, and Fe^{2+}, Mn and Mg triangular diagrams. According to Figure 4e, Fe^{2+} occupies the cubic site (i.e. chloritoids are Fe-chloritoid). The X_{Mg} values of chloritoid from these samples range from 0.09 to 0.1.

7. Mineral reactions and phase relations

For this purpose, AFM compatibility diagrams were constructed based on the actual mineral chemistry. Some samples contain the assemblage garnet,

https://doi.org/10.1017/S0016756812000209

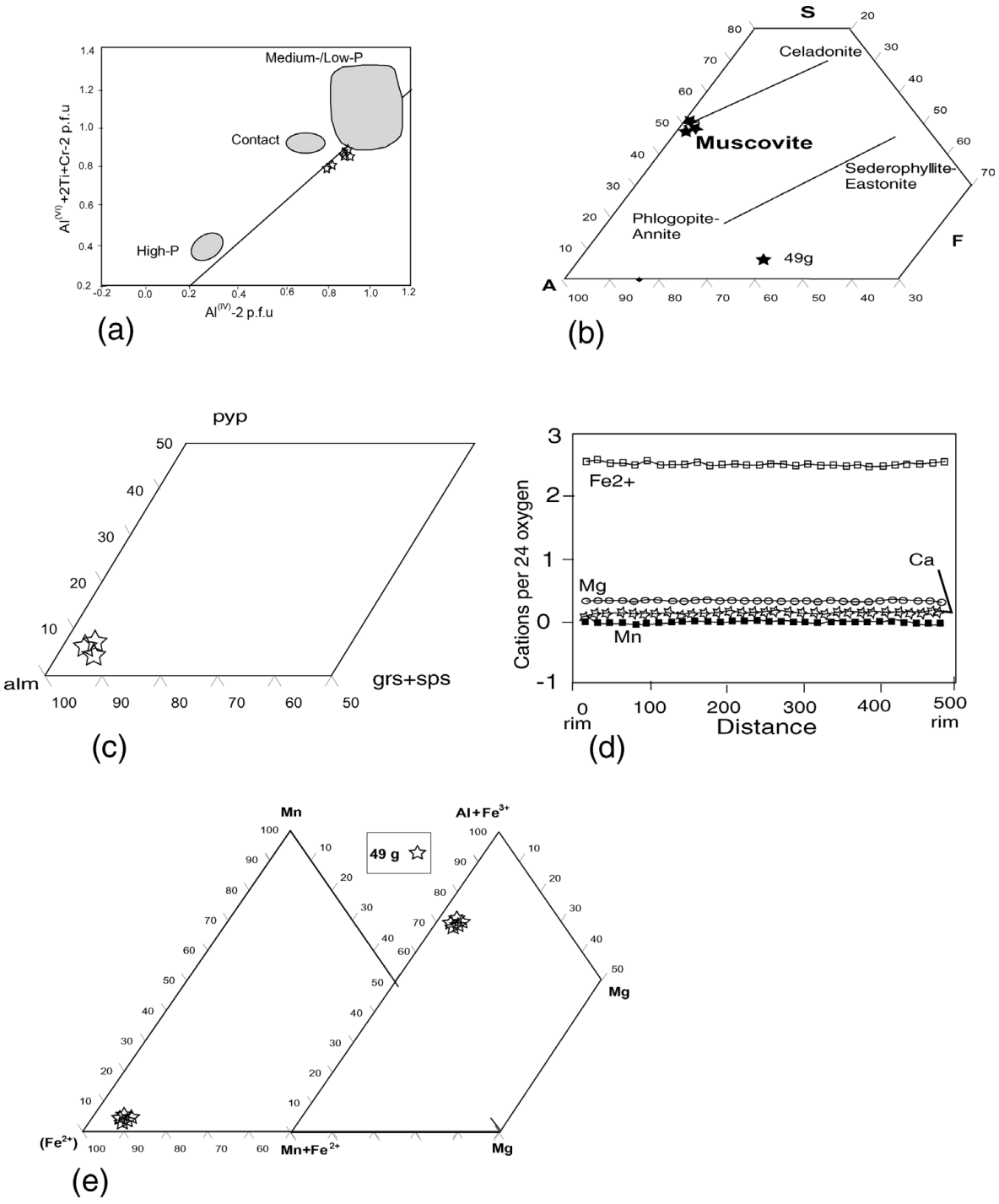

Figure 4. (a) Chlorite composition of the Poshtuk metapelites on a formula proportion diagram ($Al^{(VI)}+2Ti+Cr-2$ versus $Al^{(IV)}-2$). Compositional variation along the 1:1 line represents the Tschermak substitution. After Larid (1988). (b) Analysed white micas plotted on SAF (SiO_2, Al_2O_3, FeO) diagram. In all samples they are muscovite in composition. After Lambert (1959). (c) Composition of the studied garnets plotted on the Ca+Mn, Fe^{2+} and Mg triangular diagrams. Garnets are Fe-garnet. (d) Garnet zoning profiles from chloritoid schists of Poshtuk. Profile extends from rim to rim through the core of the garnets, which shows a flat profile. (e) Composition of the studied chloritoids plotted on the Mn, Fe^{2+}, Mg and $Mn+Fe^{2+}$, $Al+Fe^{3+}$, Mg triangular diagrams. Chloritoids are Fe-chloritoid.

staurolite, chlorite, muscovite, chloritoid and quartz. Staurolite does not coexist with biotite as it does in the classical Barrovian staurolite zone. This suggests that the bulk composition is richer in Al than common pelitic rocks. Petrographic study of the samples also shows obvious reaction rims around the garnet crystals.

7.a. The garnet-in isograd

Chloritoid is formed in the Poshtuk schists by the reaction: Fe-Chl + haematite = Ctd + magnetite + Qtz + H_2O.

In these rocks chloritoid can also act as a possible reactant for garnet formation, as can be deduced from

https://doi.org/10.1017/S0016756812000209

Table 4. Representative staurolite and garnet analyses and structural formulae

Mineral	St	St	St	St	St	Grt	Grt	Grt	Grt	Grt	Grt
	Core		Rim	Inter	Core	Core	Rim	Inter	Core	Core	Inter
SiO_2	27.40	28.20	28.15	27.60	28.60	36.80	36.40	36.40	36.00	36.30	36.75
TiO_2	0.52	0.70	0.66	0.42	0.37	0.10	0.06	0.14	0.07	0.10	0.07
Al_2O_3	57.14	56.74	56.51	57.20	56.81	20.84	20.68	20.36	21.00	20.67	21.00
Cr_2O_3	0.04	0.08	0.06	0.05	0.02	0.03	0.04	0.04	0.00	0.00	0.01
Fe_2O_3	0.00	0.00	0.00	0.00	0.00	1.47	2.34	1.51	2.18	2.17	2.05
FeO	14.24	14.40	14.72	14.50	14.07	38.25	39.13	38.76	37.5	38.37	37.70
MnO	0.07	0.15	0.15	0.16	0.14	1.35	0.44	1.37	0.54	0.90	0.70
MgO	0.32	0.30	0.31	0.33	0.30	1.37	1.50	0.57	1.83	1.22	1.78
CaO	0.00	0.01	0.00	0.01	0.00	1.57	1.02	1.91	1.65	1.60	1.87
ZnO	0.76	0.36	0.52	0.70	0.86	–	–	–	–	–	–
Na_2O	0.00	0.02	0.01	0.00	0.00	0.00	0.00	0.00	0.00	0.00	0.00
K_2O	0.01	0.00	0.01	0.01	0.01	0.00	0.00	0.00	0.00	0.00	0.00
Totals	99.76	100.96	101.0	101.0	100.86	101.76	101.58	101.03	101.02	101.32	101.92
Structural formulae on a basis of	*46 oxygen atoms*					*12 oxygen atoms*					
Si	7.46	7.60	7.60	7.48	7.71	2.96	2.94	2.96	2.94	2.94	2.94
Ti	0.106	0.14	0.13	0.08	0.07	0.00	0.00	0.01	0.00	0.00	0.00
Al	18.31	18.04	18.00	18.26	18.06	1.97	1.97	1.96	1.98	1.97	1.98
Cr	0.00	0.01	0.01	0.01	0.00	0.00	0.00	0.00	0.00	0.00	0.00
Fe(3+)	0.00	0.00	0.00	0.00	0.00	0.09	0.14	0.09	0.13	0.13	0.12
Fe(2+)	3.23	3.25	3.32	3.28	3.17	2.57	2.64	2.64	2.55	2.60	2.52
Mn	0.016	0.03	0.03	0.04	0.03	0.09	0.03	0.09	0.04	0.06	0.05
Mg	0.13	0.12	0.12	1.33	1.12	0.16	0.18	0.07	0.22	0.15	0.212
Ca	0.00	0.00	0.00	0.00	0.00	0.13	0.09	0.16	0.14	0.14	0.161
Zn	0.14	0.08	0.11	0.13	0.18	–	–	–	–	–	–
Na	0.00	0.00	0.00	0.00	0.00	0.00	0.00	0.00	0.00	0.00	0.00
K	0.00	0.00	0.00	0.00	0.00	0.00	0.00	0.00	0.00	0.00	0.00
Totals	29.41	29.30	29.36	29.43	29.36	8.00	8.00	8.00	8.00	8.00	8.00

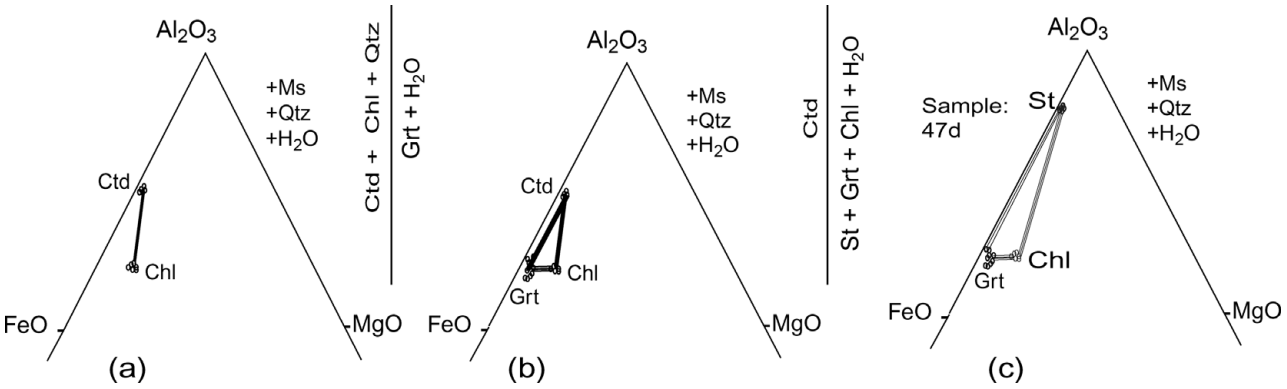

Figure 5. (a–c) Al_2O_3–FeO–MgO (AFM) projection from quartz, muscovite and H_2O of coexisting minerals in the Poshtuk schists.

the AFM-phase compatibilities (Fig. 5a–c) Fe-Ctd + Chl + Qtz = Grt + H_2O (Thomson & Norton, 1968).

7.b. The staurolite-in isograd

In the chloritoid schists, textures show that the formation of staurolite has occurred at the expense of garnet (Fig. 2e), suggesting the following reaction: Grt + Chl = St + Bt + H_2O

Figure 6a, b shows that garnet in the garnet zone samples occurs as an extra phase, stabilized by Mn. In the AFM system, the garnet zone samples (T1) are characterized by coexisting chlorite and chloritoid. At higher metamorphic temperatures (T2), the reaction: Ctd = Grt + St + Chl + H_2O results in the disappearance of chloritoid in the higher-grade rocks and the appearance of staurolite associated with continued garnet growth.

8. Geothermobarometry

The pressure and temperature of peak metamorphism is estimated using conventional thermobarometry methods such as cation exchange reaction thermometry and multiple mineral equilibria calculations. Since the chlorite–chloritoid assemblage is stable within the range of metamorphic temperatures typical for the greenschist- to blueschist facies (300–550 °C), the Fe-Mg exchange reaction between both of these minerals has good potential as a geothermometer.

For the Poshtuk chloritoid schists, the calculated temperature using the garnet-chlorite Fe-Mg exchange

https://doi.org/10.1017/S0016756812000209

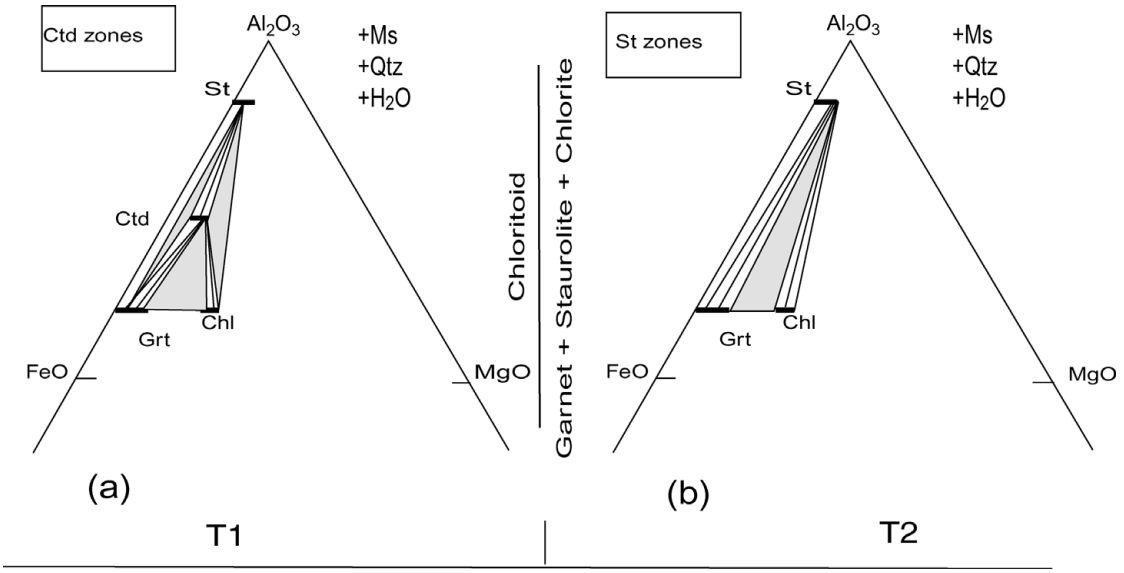

Figure 6. (a, b) AFM plots showing the mineral sub-assemblages for the garnet zone and staurolite zone samples (temperature T1 < temperature T2).

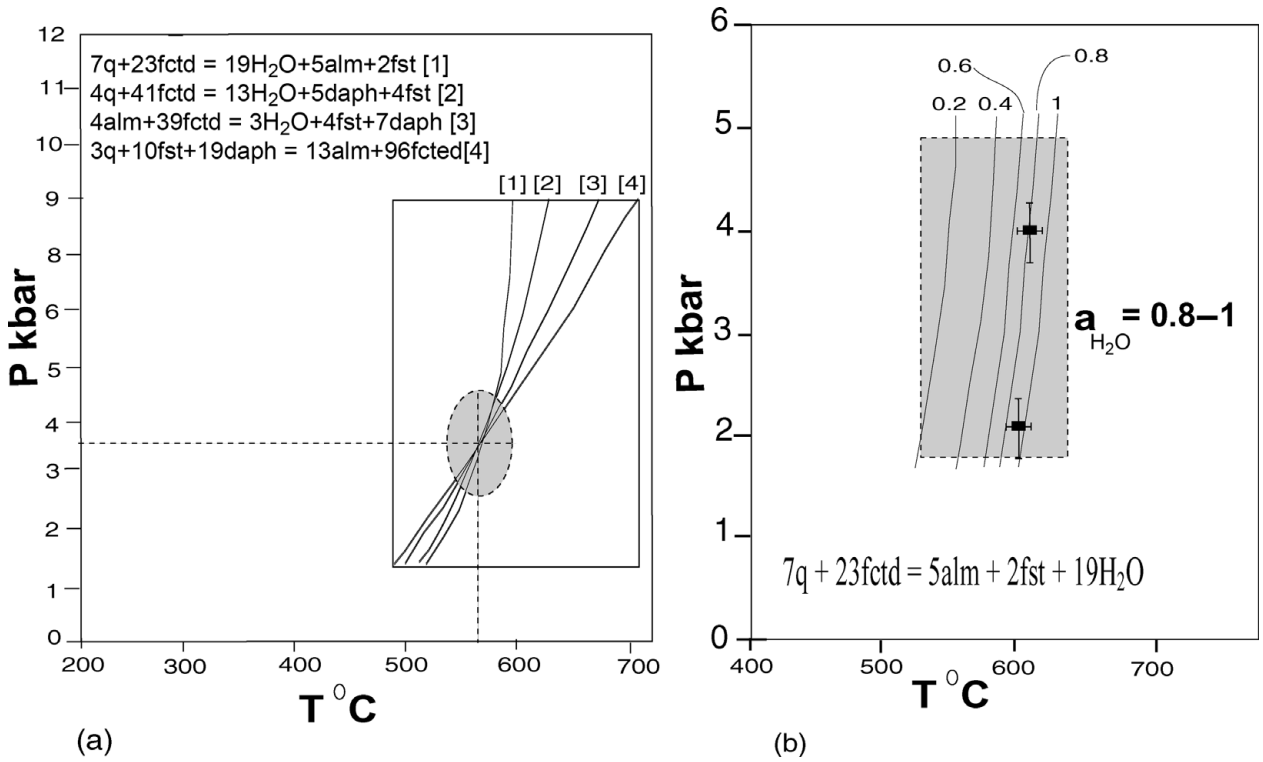

Figure 7. (a) Representative results of multiple-equilibrium calculation using the THERMOCALC (3.2) program. A pressure of ~ 3.5 kbar and temperature of ~ 570 °C can be considered for metamorphism of the Poshtuk metapelites. (b) The above *P–T* results and fluid-bearing reaction allowed us to estimate the H_2O content (0.8–1) of the fluid phase in the Poshtuk metapelite rocks.

thermometer (Grambling, 1990) is 598–635 °C. Temperatures from Fe-Mg exchange between chloritoid and chlorite (Vidal *et al*. 1999) are 533–607 °C. Furthermore, using multiple-equilibrium calculations and the THERMOCALC program, version 3.2 (Holland & Powell, 1998), temperatures and pressure were calculated using specific equilibria (Fig. 7a). Intersection of curves 1, 2, 3 and 4 in this *P–T* diagram indicate a pressure of *c*. 3.5 kbar and a temperature of 570 °C. These reactions are in agreement with the observed mineral parageneses and the AFM diagrams.

9. Discussion

Microstructural and petrographical features and field relations indicate that the formation of the Poshtuk metamorphic rocks is polymetamorphic. With respect to the flat chemical zoning profile (Fig. 4d) and the

https://doi.org/10.1017/S0016756812000209

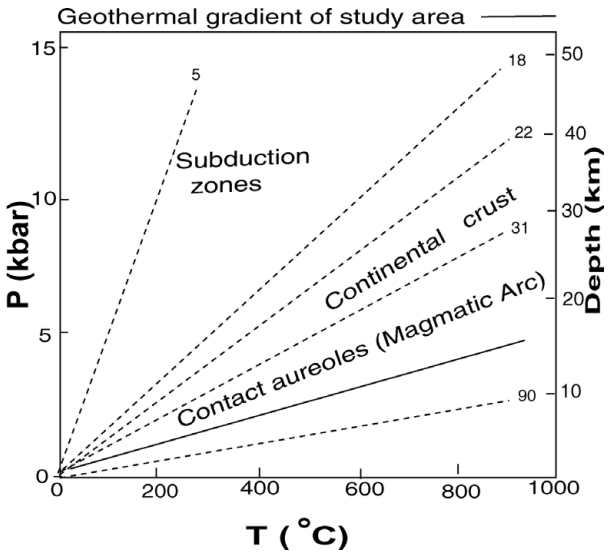

Figure 8. Simple linear temperature–depth trends for subduction, continental crust, and magmatic arc and contact aureole environments. The geothermal gradient of Poshtuk plots in the contact aureole environment.

existence of textural physical zoning in the Poshtuk garnet, different reactions among minerals and diffusion may produce apparent zonings without the existence of real chemical zoning. Contact metamorphism overprints regional metamorphism, which shows evidence for at least two deformational phases (D_1 and D_2) (Saki *et al*. 2008*a,b*). Crustal shorting and thickening is therefore accompanied by two stages of deformation (D_1 and D_2), which produced a slaty cleavage S_1 and a crenulation cleavage S_2 associated with thrusting (Saki *et al*. 2008*b*). The peak metamorphic assemblages (garnet, staurolite, chloritoid, chlorite, muscovite and quartz) grew mainly during contact metamorphism and are not typical Barrovian types. *P–T* conditions (peak metamorphic) for chloritoid schists give temperatures of 550–600 °C and pressures of 3.2–4 kbar. These *P–T* results allowed a calculation of the H_2O contents (0.8–1) of the fluid phase as shown in Figure 7b. The bulk chemistry of the metapelites indicates that their protoliths were deposited at an active continental margin. On the basis of these data, the studied rocks were at a depth of 10–12 km when they experienced the peak metamorphic temperature. This reflects a mean geothermal gradient of about 50 °C, which is typical of contact aureoles (Fig. 8). Therefore, peak metamorphism has occurred under high-temperature and low-pressure conditions (LP/HT metamorphism) and reflects the high heat flow in this part of the crust. This suggests a genetic link between granite ascent from the deep crust and the high-temperature/low-pressure (contact metamorphism) type of metamorphism in the studied area.

In the Poshtuk area, our conclusions indicate that low-*P* metamorphism (contact metamorphism) may have developed during granite emplacement that occurred during the extensive Eocene metamorphic and magmatic activities associated with the early Alpine Orogeny, which resulted in this area from the convergence between the Arabian and Eurasian plates, and the Cenozoic closure of the Tethys oceanic tract(s).

10. Conclusions

The most important results of our investigations on the metapelitic schists of the Poshtuk area, NW Iran, are:

(1) The prograde mineral assemblage garnet–staurolite–chloritoid–chlorite–muscovite is replaced by the assemblage garnet–staurolite–chlorite–muscovite close to peak metamorphism.

(2) The peak metamorphism occurred at a temperature of 580 °C and pressures of 3–4 kbar; this reflects a mean geothermal gradient of about 50 °C km^{-1}, which is typical of contact aureoles. Therefore, peak metamorphism occurred under high-temperature and low-pressure conditions (LP/HT metamorphism) and reflects the high heat flow in this part of the crust. This suggests a genetic link between granite ascent from the deep crust and the high-temperature/low-pressure (contact metamorphism) type of metamorphism in the upper crust.

(3) This metamorphism is mainly controlled by advective heat input through magmatic intrusions in the studied area. The extensive Eocene magmatic activities resulted from the convergence between the Arabian and Eurasian plates and the Cenozoic closure of the Tethys oceanic tract(s).

Acknowledgements. We thank Dr D. Rhede and Mrs O. Appelt from GFZ Potsdam, Germany for their generous help with electron microprobe analysis. Thoughtful review and invaluable comments by Dr J. Schumacher improved the paper. We appreciate editorial handling and guidance by Dr M. Allen. This work is supported by the University of Tabriz and Shahid Chamran University of Ahvaz.

References

AGARD, P., OMRANI, J., JOLIVET, L. & MOUTHEREAU, F. 2005. Convergence history across Zagros (Iran): constraints from collisional and earlier deformation. *International Journal of Earth Sciences* **94**, 401–19.

ALAVI, M. 1994. Tectonics of the Zagros orogenic belt of Iran: new data and interpretations. *Tectonophysics* **229**, 211–38.

ALAVI, M. 2004. Regional stratigraphy of the Zagros Fold-Thrust belt of Iran and its proforeland evolution. *American Journal of Science* **304**, 1–20.

ALLEN, M. B. & ARMSTRONG, H. A. 2008. Arabia–Eurasia collision and the forcing of mid-Cenozoic global cooling. *Palaeogeography, Palaeoclimatology, Palaeoecology* **265**, 252–8.

BABAKHANI, A. R. & GHALAMGHASH, J. 1990. *Geological Map of Iran, 1:100,000 series sheet Takht-e-Soleiman*. Geological Survey of Iran.

BERBERIAN, M. & KING, G. C. 1981. Towards a paleogeography and tectonic evolution of Iran. *Canadian Journal of Earth Sciences* **18**, 210–65.

DEMPSTER, T. J. & TANNER, P. W. G. 1997. The biotite isograd, Central Pyrenees: a deformation-controlled reaction. *Journal of Metamorphic Geology* **15**, 531–84.

https://doi.org/10.1017/S0016756812000209

DROOP, G. T. R. 1987. A general equation for estimating Fe^{3+} concentrations in ferromagnesian silicates and oxides from microprobe analyses using stoichiometric criteria. *Mineral Magazine* **51**, 431–5.

EFTEKHAR NEJAD, J. 1980. Tectonic classification of Iran in relation to depositional basins. *Journal of Iranian Petroleum Society* **82**, 19–28 (in Persian).

GARCIA, D., COELHO, J. & PERRIN, M. 1991. Fractionation between TiO_2 and Zr as a measure of sorting within shale and sandstone series (northern Portugal). *European Journal of Mineralogy* **3**, 401–14.

GILG, H. A., BONI, M., BALASSONE, G., ALLEN, C. R., BANKS, D. & MOORE, F. 2006. Marble-hosted sulfide ores in the Angouran Zn-(Pb–Ag) deposit, NW Iran: interaction of sedimentary brines with a metamorphic core complex. *Mineralium Deposita* **41**, 1–16.

GRAMBLING, J. 1990. Internally-consistent geothermometry and H_2O barometry in metamorphic rocks: the example garnet-chlorite-quartz. *Contribution to Mineralogy and Petrology* **105**, 617–28.

HAJIALIOGHLI, R., MOAZZEN, M., DROOP, G. T. R., OBERHÄNSLI, R., BOUSQUET, R., JAHANGIRI, A. & ZIEMANN, M. 2007. Serpentine polymorphs and P-T evolution of metaperidotites and serpentinites in the Takab area, NW Iran. *Mineralogical Magazine* **71**, 203–22.

HÄUSSINGER, H., OKRUSCH, M. & SCHEEPERS, D. 1993. Geochemistry of premetamorphic hydrothermal alteration of metasedimentary rocks associated with the Gorob massive sulfide prospect, Damara Orogen, Namibia. *Economic Geology* **88**, 72–90.

HERRON, M. M. 1988. Geochemical classification of terrigenous sands and shales from core or log data. *Journal of Sedimentary Petrology* **58**, 820–9.

HOLLAND, T. J. B. & POWELL, R. 1998. An internally consistent thermodynamic data set for phases of petrological interest. *Journal of Metamorphic Geology* **16**, 309–43.

JAMSHIDIBADR, M., COLLINS, A., MASOUDI, F., COX, G. & MOHAJJEL, M. 2011. The U-Pb age, geochemistry and tectonic significance of granitoids in The Soursat complex, Northwest Iran. *Turkish Journal of Earth Sciences*, published online 21 April 2011. doi: 10.3906/yer-1001-37.

KRETZ, R. 1983. Symbols for rock forming minerals. *American Mineralogy* **68**, 227–79.

LAIRD, J. 1988. Chlorites: metamorphic petrology. In *Hydrous Phyllosilicates* (ed. S. W. Bailey), pp. 405–53. Reviews in Mineralogy 19. Washington, DC: Mineralogical Society of America.

LAMBERT, R. ST. J. 1959. The mineralogy and metamorphism of the Moine schists of the Morar and Kroydart districts of Inverness-shire. *Transactions of the Royal Society of Edinburgh* **63**, 553.

MATHER, J. D. 1970. The biotite isograde and the lower greenschist facies in the Dalradian rocks of Scotland. *Journal of Petrology* **11**, 253–75.

MCQUARRIE, N., STOCK, J. M., VERDEL, C. & WERNICKE, B. P. 2003. Cenozoic evolution of Neo-tethys and implications for the causes of plate motions. *Geophysical Research Letters* **30**, 2036, doi: 10.1029/2003GL017992, 4 pp.

MEHRABI, B., YARDLEY, B. W. D. & CANN, J. R. 1999. Sediment-hosted disseminated gold mineralization at Zarshuran, NW Iran. *Mineralium Deposita* **34**, 673–96.

MOAZZEN, M., MOAYYED, M., MODJARRAD, M. & DARVISHI, E. 2004. Azna granitoid as an example of syn-collision S-type granitisation in Sanandaj–Sirjan metamorphic belt. Iran. *Neues Jahrbuch für Mineralogie-Monatshefte* **11**, 489–507.

MOAZZEN, M., OBERHÄNSLI, R, HAJIALIOGHLI, R., MÖLLER, A., BOUSQUET, R., DROOP, G. T. R. & JAHANGIRI, A. 2009. Peak and post-peak P–T conditions and fluid composition for scapolite-clinopyroxene-garnet calc-silicate rocks from the Takab area, NW Iran. *European Journal of Mineralogy* **21**, 149–62.

MOHAJJEL, M., FERGUSSON, C. L. & SAHANDI, M. R. 2003. Cretaceous–Tertiary convergence and continental collision, Sanandaj–Sirjan Zone, western Iran. *Journal of Asian Earth Sciences* **21**, 397–412.

NABAVI, M. H. 1976. *An Introduction to the Geology of Iran*. Tehran: Geological Survey of Iran, 109 pp (in Persian).

OTAA, T., TERABAYASHI, M. & KATAYAMA, I. 2004. Thermobaric structure and metamorphic evolution of the Iratsueclogite body in the Sanbagawa belt, central Shikoku, Japan. *Lithos* **73**, 95–126.

RAMEZANI, J. & TUCKER, R. D. 2003. The Saghand region, central Iran: U–Pb geochronology, petrogenesis and implications for Gondwana tectonics. *American Journal of Science* **303**, 622–65.

RICARDO, A. J. & MARTÍNEZ CATALÁN, R. 2003. Low-P metamorphism following a Barrovian-type evolution. Complex tectonic controls for a common transition, as deduced in the Mondoñedo thrust sheet (NW Iberian Massif). *Tectonophysics* **365**,143–64.

RICHARDS, S. W. & COLLINS, W. J. 2002. The Cooma Metamorphic Complex, a low-P, high-T (LPHT) regional aureole beneath the Murrumbidgee Batholith. *Journal of Metamorphic Geology* **20**, 119–34.

SAAD, N. A., BOUSEIL, Y. & KALIL, K. 1996. Alteration pattern in the Vmm Rugs gold mine area, Egypt. *Acta Mineralogical-Petrographica* **XXXVII**, 5–74.

SAKI, A. 2010. Proto-Tethyan remnants in northwest Iran: geochemistry of the gneisses and metapelitic rocks. *Gondwana Research* **17**, 704–14.

SAKI, A .2011. Mineralogy, geochemistry and geodynamic setting of the Mahneshan granitoids, NW Iran. *Geological Journal* **45**, 451–66.

SAKI, A., MOAZZEN, M., MODJTAHEDI, M. & OBERÄHNSLI, R. 2008*a*. Phase relations and reaction histories of chloritoid-free and chloritoid-bearing metapelites from the Mahneshan area, NW Iran. *Iranian Journal of Crystallography and Mineralogy* **16**, 622–40.

SAKI, A., MOAZZEN, M., MODJTAHEDI, M. & OBERÄHNSLI, R. 2008*b*. Determination of P-T conditions of metamorphism of Mahneshan Complex, NW Iran. *Iranian Journal of Geosciences* **68**, 80–94.

STOCKLI, D. F., HASSANZADEH, J., STOCKLI, L. D., AXEN, G., WALKER, J. D. & DEWANE, T. J. 2004. Structural and geochronological evidence for Oligo-Miocene intra-arc low-angle detachment faulting in the Takab-Zanjan area, NW Iran. *Abstracts with Programs, Geological Society of America* **36**, 319.

STOCKLIN, J. & SETUDENIA, A. 1972. *Lexique Stratigraphique International, Volume III, Asie*. Paris: Centre National de la Récherche Scientifique.

THOMSON, J. B. & NORTON, S. A. 1968. Paleozoic regional metamorphism in New England and adjacent areas. In *Studies of Appalachian Geology: Northern and Maritime* (eds E-AM, ZEN, W. S. White, J. B. Hadley & J. B. Thompson), 319–37 pp. New York: John Wiley.

TRELOAR, P. J. & O'BRIEN, P. J. 1998. Introduction. In *What Drives Metamorphism and Metamorphic*

Reactions? (eds P. J. Treloar & P. J. O'Brien), pp. 1–5. Geology Society of London, Special Publication no. 138.

VERDEL, C., WERNICKE, B. P., RAMEZANI, J., HASSANZADEH, J., RENNE, P. R. & SPELL, T. L. 2007. Geology and thermochronology of Tertiary Cordilleran-style metamorphic core complexes in the Saghand region of central Iran. *Geological Society of America Bulletin* **119**, 961–77.

VIDAL, O., GOFFE, B., BOUSQUET, R. & PARRA, T. 1999. Calibration and testing of an empiric chloritoid-chlorite Mg-Fe exchange thermometer and thermodynamic data for daphnite. *Journal of Metamorphic Geology* **17**, 25–39.

WANG, G. F., BANNO, S. & TAKEUCHI, K. 1986. Reactions to define the biotite isograde in the ryoke metamorphic belt, Kii Peninsula, Japan. *Contributions to Mineralogy and Petrology* **93**, 9–17.

https://doi.org/10.1017/S0016756812000209